

Climatology of dust days in the Central Plateau of Iran

**Tayyebah Mesbahzadeh, Ali Salajeghe,
Farshad Soleimani Sardoo, Gholamreza
Zehtabian, Abbas Ranjbar, Nir
Y. Krakauer, et al.**

Natural Hazards

ISSN 0921-030X

Volume 104

Number 2

Nat Hazards (2020) 104:1801-1817

DOI 10.1007/s11069-020-04248-6

Your article is protected by copyright and all rights are held exclusively by Springer Nature B.V.. This e-offprint is for personal use only and shall not be self-archived in electronic repositories. If you wish to self-archive your article, please use the accepted manuscript version for posting on your own website. You may further deposit the accepted manuscript version in any repository, provided it is only made publicly available 12 months after official publication or later and provided acknowledgement is given to the original source of publication and a link is inserted to the published article on Springer's website. The link must be accompanied by the following text: "The final publication is available at link.springer.com".



Climatology of dust days in the Central Plateau of Iran

Tayyebah Mesbahzadeh¹ · Ali Salajeghe¹ · Farshad Soleimani Sardoo² · Gholamreza Zehtabian¹ · Abbas Ranjbar³ · Nir Y. Krakauer⁴  · Mario Marcello Miglietta⁵ · Maryam Mirakbari¹

Received: 12 February 2020 / Accepted: 21 August 2020 / Published online: 28 August 2020
© Springer Nature B.V. 2020

Abstract

Dust storms are a major natural hazard to human health. Severe erosive storms in parts of the Central Plateau of Iran have made the situation very difficult for the inhabitants, to the extent that some areas have become depopulated. To better understand this phenomenon, dust day counts at 37 synoptic stations from 1999 to 2018 were analyzed. Dust days were most common in June, with 45% of the total number occurring in summer (June–August) and 34% in spring (March–May), and were more frequent since 2008, as compared to 1999–2007. While the spatial pattern of dust days was complex, the highest number tended to be in the southeast of the region. The stations with the most dust days, Zabol, Zahedan, and Arak, averaged 126 days, 74 days, and 73 days of dust per year, respectively. The statistical distributions that most often best fitted the time series of number of dust days (NDD) per year were Johnson SB, Log-Logistic 3-Parameter, and Burr. These fitted probability distributions were used to estimate different return period values for annual number of dust days. For example, Zabol and Sirjan stations had, respectively, the highest and lowest 2-year return period NDD values, 125 and 2 days, respectively. Overall, the spatial pattern of the NDD at different return periods indicated that southeastern Iran, as well as some northwestern and eastern portions of the study region, had particularly high values of NDD at longer return periods, while much of the northern and southwestern margins of the region have low NDD at all return periods. These results may be useful for informing the regional management of dust storms.

Keywords Number of days of dust · Frequency analysis · Return period · Central plateau of Iran

✉ Nir Y. Krakauer
mail@nirkrakauer.net

¹ University of Tehran, Tehran, Iran

² University of Jiroft, Jiroft, Iran

³ Atmospheric Science and Meteorological Research Center (ASMERC), Tehran, Iran

⁴ Department of Civil Engineering, City College of New York, New York, NY 10031, USA

⁵ Institute of Atmospheric Sciences and Climate of the Italian National Research Council (ISAC-CNR), Corso Stati Uniti 4, Padova, Italy

1 Introduction

Wind erosion is a major geomorphic process in arid and semiarid regions (Gregory et al. 2004; Buschiazzo and Zobeck 2008; Webb et al. 2009). This type of erosion involves the segregation, transport, and deposition of soil particles by winds (Li et al. 2007; Hoffmann et al. 2011). Wind erosion contributes to land degradation and desertification in arid and semiarid areas. It has a serious impact on the environment and reduces soil fertility (Schlesinger et al. 1990; Simonson 1995; Callot et al. 2000; Prospero 2002; Peterson et al. 2006). This type of erosion can be aggravated by erosive agents (Gill 1996; Marticorena et al. 1997; Belnap and Gillette 1998; Okin et al. 2001, 2006) which include soil dryness and lack of vegetation cover as well as wind intensity. Airborne dust is a consequence of wind erosion in affected areas. Dust commonly has major impacts on climate, human health, air quality, and the environment in desert areas (Schwartz 1994; Overpeck et al. 1996; Goudie and Middleton 2001; Husar et al. 2001; Shao and Dong 2006; Ginoux et al. 2012; Goudie 2014). Dust storms also have a significant impact on the Earth's radiation budget, global biogeochemical cycles, soil composition, and atmospheric chemistry (Chadwick et al. 1999; Reynolds et al. 2001; Jickells 2005; Alfaro 2008; Chappell et al. 2012). The amount of atmospheric dust is affected by rainfall, wind intensity, regional moisture balance, and man-made dust sources. Increases in the amount of atmospheric dust and loss of vegetation in arid and semiarid areas can cause global cooling (Crucifix and Hewitt 2005; Schneider von Deimling et al. 2006). In Iran, dust is a major hazard due to the arid and semiarid climate covering almost 75% of the country, and particularly the desert source regions of Lut desert and Kavir plain. This phenomenon has led to very poor air quality and serious health impacts (Ghaljahi et al. 2019) and even forced out-migration causing depopulation of some areas, notably in southeastern and southwestern Iran (Smyth 2018; Khavarian-Garmsir et al. 2019). One obvious impact of dust storms in these areas is related to the reduction of horizontal visibility. Visibility can be reduced to several meters, which causes road accidents. The World Meteorological Organization (WMO) categorizes dust events based on horizontal visibility: blowing dust is characterized by horizontal visibility of 1 to 10 kilometers, sand and dust storm conditions have visibility under 1 kilometer, and severe sand and dust storm conditions have horizontal visibility under 500 meters (UNEP et al. 2016). Middleton (2017) offers a comprehensive account of hazards related to dryland dust entrainment, transport, and deposition.

In recent years, extensive research has been conducted on dust storms (Shao and Wang 2003), often based on numerical models (Shao et al. 2003; Park 2003), remote sensing data (Prospero 2002; Kaskaoutis et al. 2007), and geographic information systems. The spatial and temporal characteristics of these storms are widely studied, since the frequency of dust events is an indicator of environmental change, including desertification processes, changes in vegetation coverage, and the impact of human activities in arid and semiarid regions (Gao et al. 1997; Goudie and Middleton 2001).

The return period is the average time interval between occurrences of a phenomenon and is used to describe the severity and frequency of natural disasters (Liu et al. 2015). In particular, the return period is widely used in the assessment of natural disaster risk in hydrology and meteorology areas, as well as in infrastructure design, planning and project management (Iqbal and Ali 2012) and in creating effective early warning systems and carrying out necessary control measures based on the mechanisms of storm formation and needs for monitoring (Berkhout et al. 2006).

The purpose of this study was to examine the spatial and temporal pattern of dust days in the Central Plateau region of Iran and estimate return periods for number of dust days per year. Dust day occurrence was evaluated based on codes recorded at weather stations in this region.

2 Methods

2.1 Area of study

The Central Plateau is the largest physiographic region in Iran and includes the deserts of the Kavir and Lut Plains. It is a warm and arid region that covers over 824,000 km², accounting for 51% of Iran's total area. The Plateau averages 1300 meters above sea level. However, altitude in the desert lowers to 700 m, and in parts of the Lut Desert even to 300 m. The Alborz and Zagros Mountains prevent Mediterranean moisture from entering the area (Ghorbani 2013). Hence, rainfall is low, with an annual average of less than 100 mm, and as little as 25 mm in some locations.

On the contrary, potential evaporation in this area is high and in many cases reaches over 4000 mm/year. As such, evaporation can reach more than 40 to 80 times the annual rainfall (Azadi et al. 2015). The average relative humidity is 30 to 40 percent, but decreases to 15 percent during the warm season. The mean annual temperature varies between 15 and 30 degrees Celsius, and the maximum and minimum temperatures are reported to be 51 and −18 °C, respectively (Naderi and Raeisi 2015). One of the most pressing problems in the region is the phenomenon of dust storms that annually cause irreparable damage to human communities, infrastructure, and natural ecosystems. Dry climate, low vegetation, erosive winds, and low soil moisture are the main causes of dust occurrence. Figure 1 shows the geographical location of the weather stations studied here in the region and as part of Iran.

2.2 Data used

The study used data from 37 synoptic weather stations that had a common 20-year record period from 1999 to 2018. Out of the 100 meteorological codes (00 to 99) defined by the WMO in their WW (present weather) series, 11 codes are associated with dust events, as shown in Table 1. Table 2 gives information about the stations. For each station, the number of days of dust (NDD) per calendar year was extracted for the period 1999 to 2018 and visualized.

2.3 Spatial analysis of NDD

After the mean NDD per year at the selected synoptic stations was calculated (Table 3), interpolation was used in order to visualize the spatial pattern of dust in the study area. Inverse distance weighting (IDW) (Eq. 1), which is one of the most commonly used spatial interpolation methods, was chosen to map the NDD in ArcGIS 10.5 software. The formula for IDW is

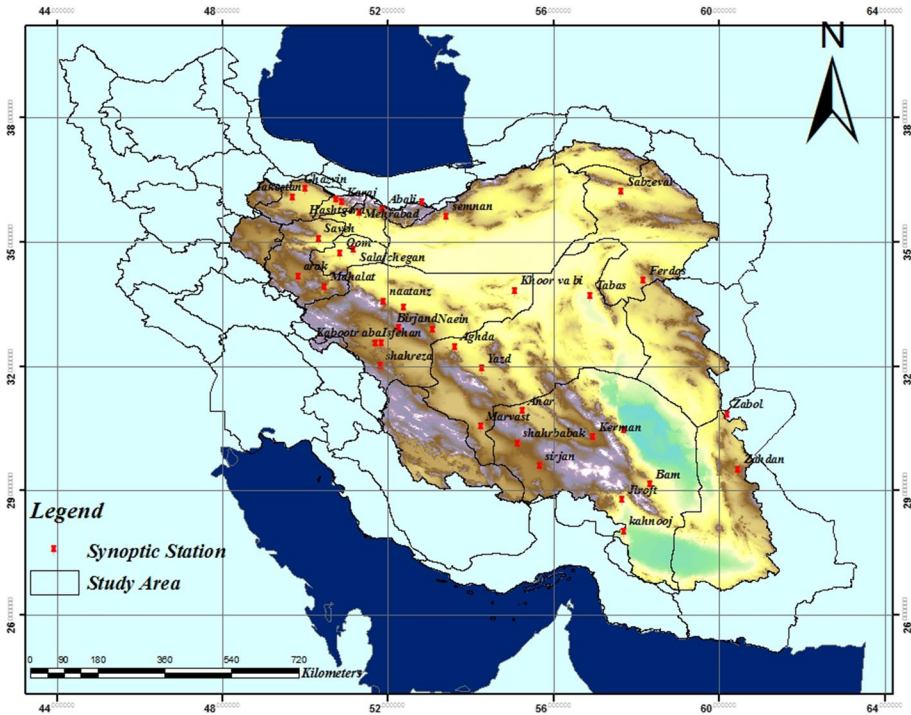


Fig. 1 Location of weather stations. Colors indicate elevation within Iran’s Central Plateau (the study area)

Table 1 Phenomena related to dust according to the WMO weather codes Kamal et al. (2019)

Synoptic code	Weather description
06	Widespread dust in suspension in the air, not raised by wind at or near the station at the time of observation
07	Well-developed dust or sand whirl seen at or near the station during the preceding hour or at the time of observation, but no dust storm or sandstorm seen
08	Well-developed dust or sand whirl seen at or near the station during the preceding hour or at the time of observation, but no dust storm or sandstorm.
09	Dust storm or sandstorm within sight at the time of observation or at the station during the preceding hour
30–32	Slight or moderate dust storm or sandstorm
33–36	Severe dust storm or sandstorm
98	Thunderstorm combined with dust storms or sandstorms at time of observation

Table 2 Location of the synoptic weather stations used

	Station	Latitude (°)	Longitude (°)	Elevation(m)
1	Anar	30.88	55.25	1409
2	Bam	29.10	58.35	1066.9
3	Jiroft	28.73	57.67	775
4	Kahnooj	27.97	57.70	499
5	Kerman	30.25	56.97	1754
6	Shahdad	30.42	57.70	482
7	Sirjan	29.55	55.68	1767
8	ShahrBabak	30.10	55.13	1834.1
9	Ardestan	33.38	52.38	1255.5
10	Isfahan	32.52	51.71	1550.4
11	Khoor va Biabank	33.78	55.08	842.2
12	Naein	32.85	53.08	1573.7
13	Natanz	33.53	51.90	1685
14	Shahr Reza	31.98	51.83	1858
15	Kabootar Abad	32.52	51.85	1542.5
16	Arak	34.13	49.83	1661.9
17	Mahalat	33.88	50.48	1622
18	Saveh	35.05	50.33	1111.6
19	Qom	34.70	50.85	879.1
20	Salafchegan	34.78	51.18	853
21	Semnan	35.59	53.42	1127
22	Zabol	30.80	60.20	489.2
23	Zahedan	29.47	60.47	1370
24	Aghda	32.43	53.62	1150
25	Yazd	31.90	54.28	1230.2
26	Marvast	30.50	54.25	1547
27	Sabzevar	36.18	57.65	1858
28	Birjand	32.89	52.28	1491
29	Fedoos	34.03	58.18	1293
30	Tabas	33.67	56.90	690
31	Karaj	35.92	50.90	1292.9
32	Hashtgerd	36.00	50.75	1612.9
33	Ghazvin	36.25	50.00	1279.1
34	Takestan	36.05	49.70	1283.4
35	MehraBad	35.68	51.32	1191
36	Abali	35.75	51.88	2465.2
37	Firoozkooh	35.92	52.83	1976

Table 3 NDD statistics by weather station

	Station	Mean	SD	Skew	Min.	Max.
1	Anar	22.25	14.06	1.24	5	61
2	Bam	45.75	45.32	1.76	5	174
3	Jiroft	26.75	20.71	1.07	6	76
4	Kahnooj	19.1	14.60	1.48	2	61
5	Kerman	27.15	16.64	1.49	12	72
6	Shahdad	18.05	14.18	1.86	1	64
7	Sirjan	17.05	19.75	2.41	1	85
8	ShahrBabak	15.05	9.53	1.08	3	36
9	Ardestan	40.25	25.08	0.10	3	81
10	Isfahan	33.05	22.93	0.044	1	65
11	Khoor va Biabank	41.8	26.30	0.164	7	85
12	Naein	43.9	26.08	0.63	9	101
13	Natanz	27.01	16.20	0.014	3	52
14	Shahr Reza	27.90	19.45	0.77	5	71
15	Kabootar Abad	23.60	18.72	1.17	3	72
16	Arak	73.05	24.93	0.01	26	112
17	Mahalat	46.55	30.33	0.52	10	98
18	Saveh	59.05	35.54	0.28	13	121
19	Qom	52	36.722	0.636	12	121
20	Salafchegan	46	27.50	0.47	6	98
21	Semnan	15.05	13.40	2.28	1	61
22	Zabol	126.5	21.25	0.001	87	164
23	Zahedan	74.75	18.99	-0.58	37	102
24	Aghda	23	14.38	0.18	2	47
25	Yazd	55.35	25.75	0.28	21	96
26	Marvast	17.35	10.47	1.20	4	45
27	Sabzevar	16.5	8.65	1.83	5	45
28	Birjand	25.95	18.23	0.97	6	70
29	Fedoos	12.95	9.95	1.65	2	42
30	Tabas	61.65	21.32	1.05	25	135
31	Karaj	18.05	18.72	1.95	2	78
32	Hashtgerd	8.35	10.21	2.26	1	42
33	Ghazvin	6.9	3.14	0.32	2	12
34	Takestan	4.45	3.0	1.46	1	15
35	MehraBad	16.8	5.16	0.01	7	26
36	Abali	7.1	5.07	1.41	2	21
37	Firoozkooh	8.55	8.26	1.94	1	34

NDD number of dust days per year; *SD* standard deviation; *Skew* skewness; *Min* minimum; *Max* maximum

$$Z_j = \frac{\sum_{i=1}^n \frac{z_i}{d_{i,j}^a}}{\sum_{i=1}^n \frac{1}{d_{i,j}^a}}, \quad (1)$$

where $d_{i,j}$ is the distance between the estimation point and each of the neighboring samples, Z_j is the value of the parameter estimated at point j , z_i is the value of the parameter observed at point i , and a is the power of inverse distance (kept at a default value of 2).

2.4 Frequency analysis of NDD

Frequency analysis is a statistical method used to estimate the probability of occurrence of extreme phenomena. The primary purpose of frequency analysis is to relate the magnitude of the extreme events to their frequency through the use of statistical distributions. Understanding the frequency of events such as dust can be useful in providing management strategies to reduce impact. Frequency analysis can be performed to determine the return period of an extreme event. Also, based on the results of frequency analysis, the expected event value can be estimated for different return periods. Therefore, in this study, frequency analysis of dust events used to calculate 2-, 5-, 10-, 25-, 50-, and 100-year return periods for NDD at each station. The p -year return period value corresponds to the value of the $1 - 1/p$ quantile of the cumulative distribution function (CDF) of annual NDD. This CDF is estimated by fitting several candidate univariate probability distribution functions to each station's time series of annual NDD and selecting the best-fitting one in each station. The goodness of fit of each candidate distribution to the data is quantified using the Akaike information criterion (AIC), a widely applicable model selection tool which combines the likelihood of the data given the model with the number of fitted parameters; for each station, the distribution with lowest AIC value was chosen (Akaike 1974; Burnham and Anderson 2004). The selected probability distributions for NDD at each station and their associated parameters are shown in Table 4. Using instead as the goodness of fit criterion a combination of Kolmogorov–Smirnov and Anderson–Darling test statistics as implemented in EasyFit5.5 Professional software (Modaresi Rad et al. 2016) also led to the same distributions being chosen.

3 Results

3.1 Mean and temporal pattern of NDD

Zabol and Zahedan stations, in the southeast of the study area, had the highest average NDD, with 126 and 74 dust days, respectively, per year (Table 3). One of the most important reasons for these conditions is the existence of monsoon winds in Sistan for some 120 days per year (Alizadeh-Choobari et al. 2014). In the central part of the study area, Yazd and Nain stations, with 56 and 45 days, had the highest average NDD. In the east of the study area, Tabas station with 63 days has the highest average NDD. In the north, Karaj station, with 20 days, and in the northwest, Arak station, with 73 days, had the highest NDD. In the west of the study area, Reza station had the highest mean NDD of 29. For the region as a whole, the average NDD does not show neat spatial patterns, though the southeastern part (around Zabol station) has the most dust overall, with another area of high NDD in the northwest (around Arak station; Fig. 2).

Table 4 Best statistical distribution for number of dust days at each station and the values of the parameters of each distribution

Station	Fitted distribution	Parameters
1 Anar	Burr	$\kappa = 2.1056, \alpha = 2.2582, \beta = 29.374$
2 Bam	Burr	$\kappa = 0.65893, \alpha = 2.3531, \beta = 22.217$
3 Jiroft	Johnson SB	$\gamma = 0.90877, \delta = 0.5619, \lambda = 83.536, \xi = 5.3182$
4 Kahnooj	Log-Logistic (3P)	$\alpha = 2.3737, \beta = 15.572, \gamma = -0.61448$
5 Kerman	Frechet	$\alpha = 2.2684, \beta = 17.587$
6 Shahdad	Log-Logistic (3P)	$\alpha = 2.8996, \beta = 18.155, \gamma = -3.5198$
7 Sirjan	Pareto	$\alpha = 0.44692, \beta = 1$
8 ShahrBabak	Burr (4P)	$\kappa = 360.13, \alpha = 1.2737, \beta = 1344.9, \gamma = 2.7231$
9 Ardestan	Johnson SB	$\gamma = 0.44998, \delta = 0.32237, \lambda = 104.61, \xi = 15.628$
10 Isfahan	Beta	$\alpha_1 = 0.47403, \alpha_2 = 0.47255, \alpha = 1.0, \beta = 65.0$
11 Khoor va Biabank	Johnson SB	$\gamma = 0.12999, \delta = 0.42765, \lambda = 78.644, \xi = 5.7507$
12 Naein	Johnson SB	$\gamma = 0.93061, \delta = 1.0609, \lambda = 145.08, \xi = -2.9241$
13 Natanz	Beta	$\alpha_1 = 0.63246, \alpha_2 = 0.65346, \alpha = 3.0, \beta = 52.0$
14 Shahr Reza	Johnson SB	$\gamma = 0.80509, \delta = 0.73837, \lambda = 85.644, \xi = 1.5947$
15 Kabootar Abad	Gamma	$\alpha = 1.5878, \beta = 14.864$
16 Arak	Uniform	$\alpha = 29.862, \beta = 116.24$
17 Mahalat	Gen. Pareto	$\kappa = -0.40108, \sigma = 58.668, \mu = 4.6765$
18 Saveh	Johnson SB	$\gamma = 0.18714, \delta = 0.19416, \lambda = 97.574, \xi = 17.559$
19 Qom	Johnson SB	$\gamma = 0.44998, \delta = 0.32237, \lambda = 104.61, \xi = 15.628$
20 Salafchegan	Log-Pearson 3	$\alpha = 4.0706, \beta = 63.158, \gamma = -21.78$
21 Semnan	Log-Logistic (3P)	$\alpha = 2.5061, \beta = 13.27, \gamma = -1.7274$
22 Zabol	Gamma	$\alpha = 35.46, \beta = 3.5688$
23 Zahedan	Gen. Extreme Value	$\kappa = -0.56447, \sigma = 21.376, \mu = 70.585$
24 Aghda	Johnson SB	$\gamma = 0.15973, \delta = 0.50978, \lambda = 46.52, \xi = 1.9671$
25 Yazd	Gen. Pareto	$\kappa = -0.62164, \sigma = 63.648, \mu = 16.101$
26 Marvast	Log-Gamma	$\alpha = 20.121, \beta = 0.13358$
27 Sabzevar	Inv. Gaussian (3P)	$\lambda = 83.375, \mu = 17.761, \gamma = -1.261$
28 Birjand	Johnson SB	$\gamma = 0.88881, \delta = 0.62717, \lambda = 76.744, \xi = 5.0807$
29 Fedoos	Log-Pearson 3	$\alpha = 720.66, \beta = -0.02752, \gamma = 22.14$
30 Tabas	Log-Logistic (3P)	$\alpha = 1.5031, \beta = 24.326, \gamma = 23.631$
31 Karaj	Burr	$\kappa = 3.0156, \alpha = 1.2589, \beta = 35.833$
32 Hashtgerd	Johnson SB	$\gamma = 1.8033, \delta = 0.63767, \lambda = 69.629, \xi = 0.41534$
33 Ghazvin	Rayleigh	$\sigma = 5.5054$
34 Takestan	Weibull (3P)	$\alpha = 0.84251, \beta = 3.2905, \gamma = 1.0$
35 MehraBad	Pearson 6 (4P)	$\alpha_1 = 7.6489, \alpha_2 = 9.2582 \times 10^7, \beta = 1.8762 \times 10^8, \gamma = 1.4112$
36 Abali	Rayleigh	$\sigma = 5.5054$
37 Firoozkooh	Log-Logistic (3P)	$\alpha = 1.6742, \beta = 5.2417, \gamma = 0.46257$

P number of parameters; *Gen.* generalized; *Inv.* inverse

Most of the stations showed high interannual variability in NDD (over half of the mean value) and positive skewness (Table 3). The map of maximum annual NDD across the study period (Fig. 3) shows that the southeast, east, and northwestern sections show higher peak NDD, indicating the concentration of dust in these areas. The maximum

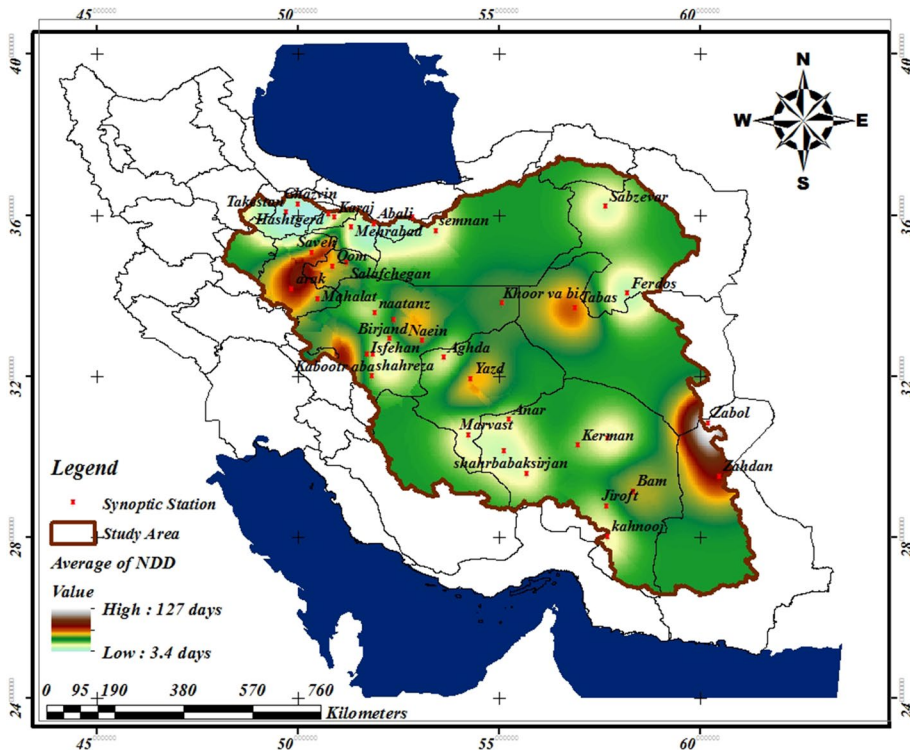


Fig. 2 Interpolated surface of mean NDD per year

dust days at Bam station, with 174 days in 2008, Zabol station, with 164 days in 2017, as well as Tabas station, with 135 days of dust in 2009, were the highest NDD found in the study area (Table 3).

The spatial pattern of minimum NDD in the study area (Fig. 4) showed that the southeastern part of the study area has very high minimum NDD. Zabol station, located there, had the highest minimum value of 87 days of dust in 2002, the minimum year. Zahedan station was next, with a minimum of 37 dust days in 2000.

All the stations in the study area had at least 1 day of dust each year in 1999–2018 (Table 3). However, averaging across stations, there was a threefold variation between years in mean NDD, ranging from a minimum of 17.0 days in 2000 to a maximum of 50.5 days in 2008. After 2008, the years with next highest mean NDD were 2012 (48.0 days), 2015 (47.6), and 2018 (45.4), reflecting a tendency for frequent dust occurrence over the later part of the study period (Fig. 5). In fact, the nonparametric Mann–Kendall test shows that the increase in mean NDD over the study period is highly statistically significant ($p < 0.001$).

NDD showed pronounced seasonality, with dust days being most common in June, followed by July, and least common in December, followed by November (Fig. 6). Some 45% of the total number of dust days, summed across stations, occurred in meteorological summer (June–August) and 34% in spring (March–May), compared with only 12% in fall (September–November) and 9% in winter (December–February).

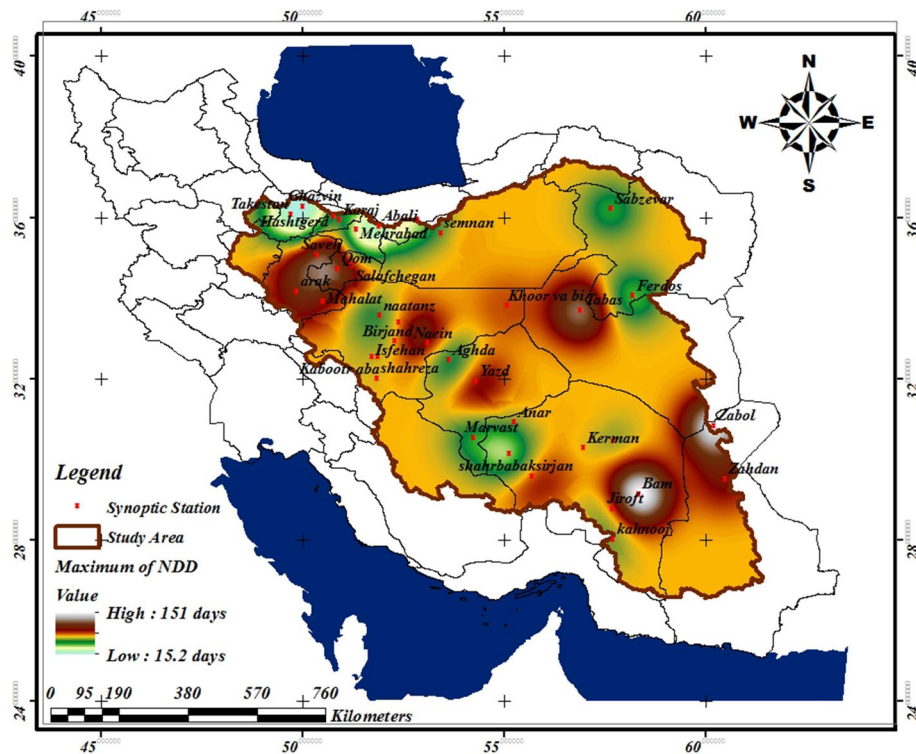


Fig. 3 Interpolated surface of maximum annual NDD over 1999–2018

3.2 NDD return periods

To analyze the frequency of dust days and to calculate their return period, AIC was used as a goodness-of-fit criterion to choose the most appropriate statistical distribution function for the annual NDD time series at each station. The parameters of each fitted distribution function were extracted to determine the NDD with different return periods. The results are shown in Table 4. The Johnson SB distribution function was selected for 10 out of the 37 stations, while the Log-Logistic 3P distribution function was selected 5 times, and several other distributions were selected less frequently.

Using the selected statistical distribution functions for each station, the number of days of dust at the return periods of 2, 5, 10, 25, 50, and 100 years was predicted. The results showed that, for example, at the 2-year return period, Zabol station had the maximum value for the annual number of dust days, 125. After Zabol station, Zahedan, Arak and Yazd stations ranked next, with 79, 73, and 58 days of dust, respectively, estimated for the 2-year return period.

The spatial pattern of dust days in different return periods indicates that the largest number of dust days at different return periods is mostly in the southeast, northwest, and center of the study region. Zabol, Zahedan, and Arak stations were among the dustiest. The zoning of this phenomenon over the 5-year return period has a more regular spatial pattern, as the southeastern and northwestern regions have maximum dust events, and as we move

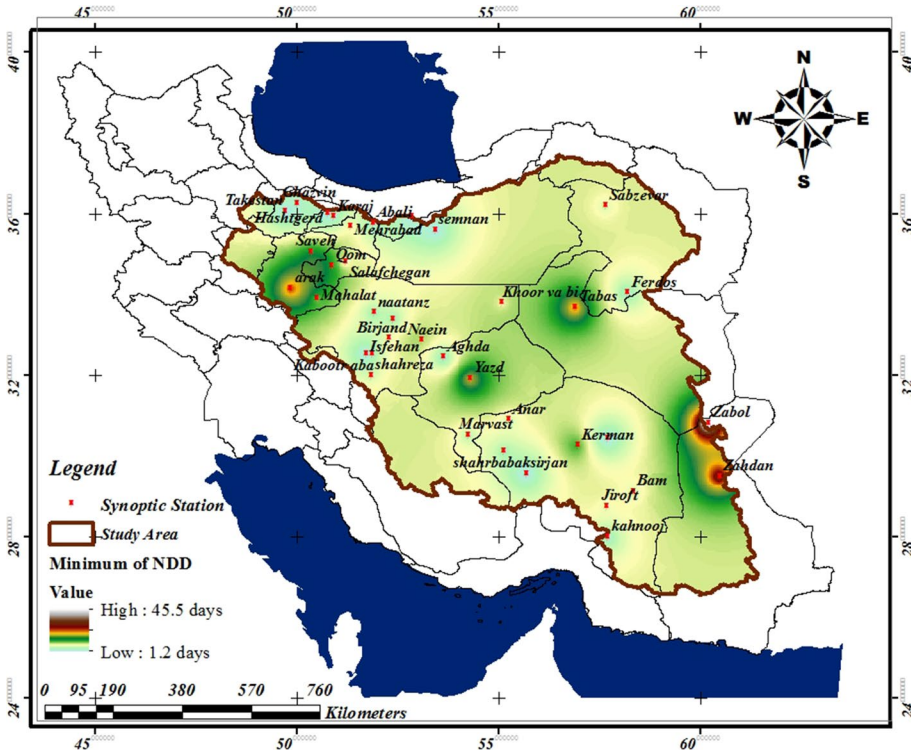
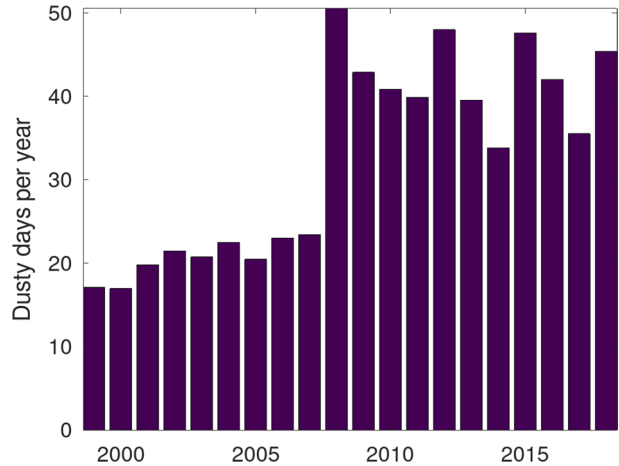


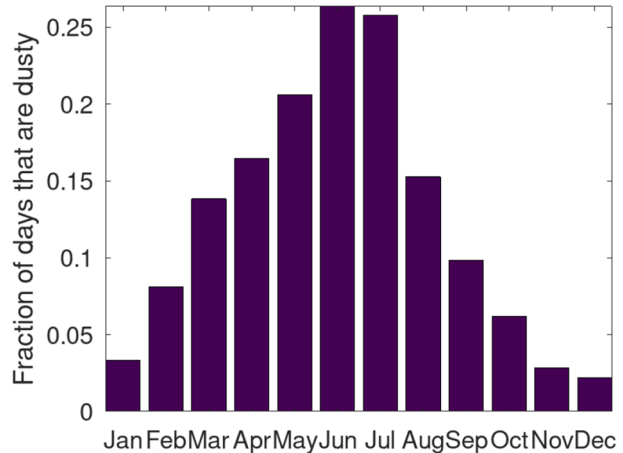
Fig. 4 Interpolated surface of minimum annual NDD over 1999–2018

Fig. 5 NDD per year over 1999–2018, averaged over the 37 weather stations



toward the center of the region, the number of events decreases. In the northern and southern parts of the region, the number of dust days at the 5-year return period is also lower. Analysis of the range of dust days over the 10-year return period indicates that the southeastern parts will have the highest occurrence of dust, but the concentration of dust days in

Fig. 6 Fraction of days each month with recorded dust over 1999–2018, averaged over the 37 weather stations



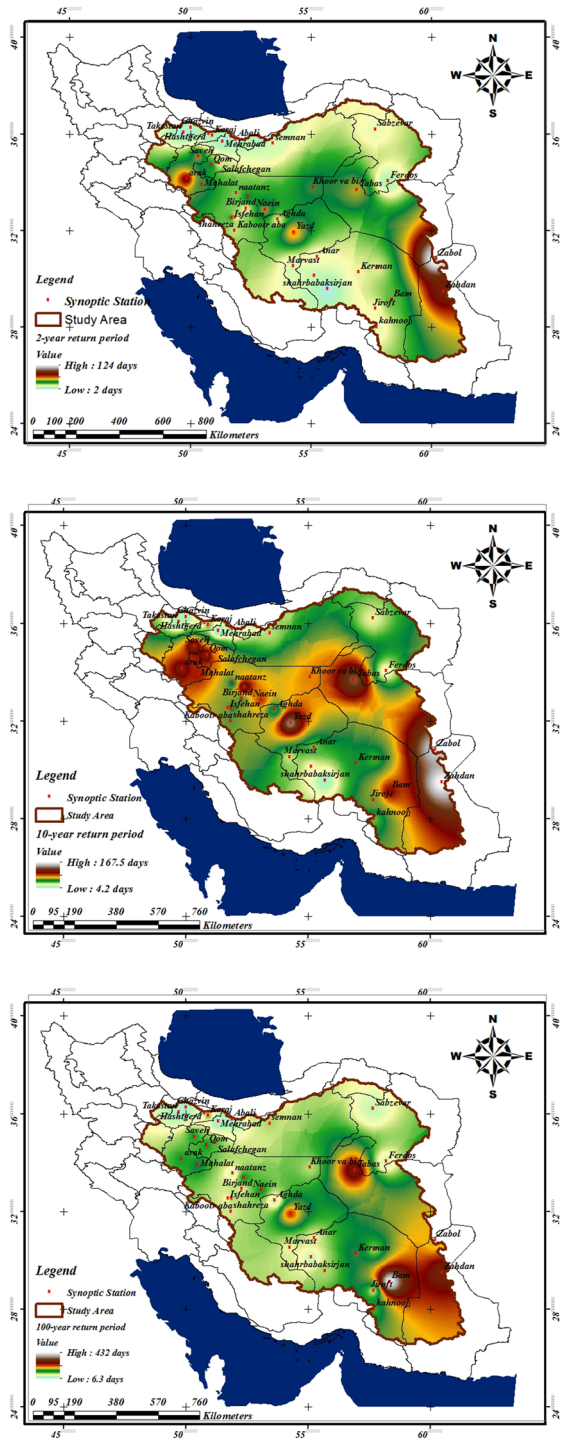
the center is greater than the northwest. For example, using the 10-year return period, Yazd station with 138 dust days and Saveh stations with 115 dust days and Qom station with 113 dust days are identified as areas of high vulnerability in the center of the study area. Zonation of dust days at the 25-, 50-, and 100-year return periods indicates higher NDD from the northwest and center to the east of the region. The southeastern part has the most NDD at all return periods, but the location of the maximum shifts from the far southeast (Zabol) at 2 years to further south, north, and west (e.g., Zahedan, Bam, and Tabas stations) at 10 years and longer. Figure 7 illustrates the interpolated NDD at 2-, 10-, and 100-year return periods over the study area.

4 Discussion and conclusion

In much of Iran and elsewhere, the dust phenomenon is a major challenge for public health. The phenomenon is the result of wind erosion and part a process of desertification and land degradation, and can threaten human infrastructure and leave areas uninhabited. In this study, statistical methods were used to analyze this phenomenon and study its spatial and temporal pattern. Results show that southeastern part of Iran's Central Plateau, including Zabol and Zahedan stations, has the highest rate of dust occurrence. One of the main causes of dust in this area is the 120-day winds of Sistan, which are very fast and very hot, in the late spring to early fall (Alizadeh-Choobari et al. 2014). Strong winds and low humidity frequently cause dust lofting (Rashki et al. 2012). This has severe economic and social impacts on the lives of the residents there and also threatens their health (Miri et al. 2009; Ghaljahi et al. 2019). The Hirmand Wetland on the border between Iran and Afghanistan is one major source of dust in the dry season (Middleton 1986, 2019).

The results also show that most of the dust events occur in the spring and summer. Chun et al. (2001) and Shao and Dong (2006) found that dust storms in parts of China, Korea, Japan, and other parts of eastern Asia occur in the spring, similar to the results of this study in the central Iranian plateau. June, July, May, and April were the months with most frequent dust days. The spatial pattern of this phenomenon indicates that the number of dust days does not follow a simple pattern, but parts of the southeast and northwest of the study area had the highest number of dust days. The finding that the southeastern region of Iran's

Fig. 7 Interpolated surface of estimated NDD at various return periods: **a** 2 years, **b** 10 years, **c** 100 years



Central Plateau has the highest frequency of dust confirms previous studies (e.g., Cao et al. 2015; Modarres and Sadeghi 2017; Middleton 2019; Baghbanan et al. 2019). The geographic and seasonal patterns of dust storms relate to the distribution of dust source areas inside and outside Iran, as well as to local and regional synoptic conditions that govern dust transport (Rashki et al. 2015; Mesbahzadeh et al. 2020a, b). These are in turn affected by anthropogenic water withdrawals and land degradation, as well as by soil drying and vegetation loss due to climate change (Nouri et al. 2019; Mirakbari et al. 2020).

The main contribution of the current study is in analyzing the probability distribution of annual NDD and computing the distribution of NDD values at different return periods across the Central Plateau of Iran. The best distribution function of each station was selected by using a goodness of fit criterion. The Johnson SB distribution function, fitted to observational data at ten stations, was the most frequently selected as the most appropriate function. Dust days were calculated for the 2-, 5-, 10-, 25-, 50- and 100-year return periods. Averaged across all the stations, NDD was 28 at the 2-year return period, rising to 50 days per year at the 5-year return period and 62 days at the 10-year return period. Overall, the spatial pattern of the number of days of dust during different return periods indicated that southeastern Iran as well as some northwestern and eastern portions of the study region had particularly high values of NDD at longer return periods. The central Iranian pattern was more regular, in that it is always moderate in the number of days of dust, while much of the northern and southwestern margins of the Central Plateau region have low NDD at all return periods.

There are a number of limitations in our research that should be kept in mind when interpreting it and could be addressed in future work. We did not distinguish different levels of dust storm severity or set specific visibility thresholds in compiling NDD data from station reports. Considering the distribution of different weather codes separately could provide insight into whether the distribution of severe dust storm days could be different from that of moderate dust days. We also did not analyze how the fit of NDD series to different probability distributions corresponds to differences in the physiographic, meteorologic, or other characteristics of stations that pattern interannual variability in dust phenomena. As well, the fitted probability distributions and associated return periods do not take into account temporal change in propensity for dust storms; risks under future climate and land use may in fact be different.

Overall, the differences in mapped values across return periods distinguish areas where the mean NDD is high but the interannual variation may be low (which have the highest NDD at short return periods) from those where the mean may be lower while interannual variation is high (which have relatively more NDD at long return periods). Such distinctions may be helpful for managing dust storm hazards, particularly given the predominance of years with heavy dust loading since 2008.

Compliance with ethical standards

Conflict of interest The authors declare that they have no conflict of interest.

References

Akaike H (1974) A new look at the statistical model identification. *IEEE Trans Autom Control* 19(6):716–723. <https://doi.org/10.1109/tac.1974.1100705>

- Alfaro SC (2008) Influence of soil texture on the binding energies of fine mineral dust particles potentially released by wind erosion. *Geomorphology* 93(3–4):157–167. <https://doi.org/10.1016/j.geomorph.2007.02.012>
- Alizadeh-Chooabari O, Zavar-Reza P, Sturman A (2014) The “wind of 120 days” and dust storm activity over the Sistan basin. *Atmos Res* 143:328–341. <https://doi.org/10.1016/j.atmosres.2014.02.001>
- Azadi S, Soltani Kopaei S, Faramarzi M, Soltani Tudehski A, Pourmanafi S (2015) Evaluation of Palmer drought severity index in central Iran. *J Water Soil Sci* 19(72):305–319. <https://doi.org/10.18869/acadpub.jstnar.19.72.26>
- Baghbanan P, Ghavidel Y, Farajzadeh M (2019) Spatial analysis of spring dust storms hazard in Iran. *Theor Appl Climatol*. <https://doi.org/10.1007/s00704-019-03060-y>
- Belnap J, Gillette DA (1998) Vulnerability of desert biological soil crusts to wind erosion: the influences of crust development, soil texture, and disturbance. *J Arid Environ* 39(2):133–142. <https://doi.org/10.1006/jare.1998.0388>
- Berkhout F, Hertin J, Gann DM (2006) Learning to adapt: organisational adaptation to climate change impacts. *Clim Change* 78(1):135–156. <https://doi.org/10.1007/s10584-006-9089-3>
- Burnham KP, Anderson DR (2004) Multimodel inference: understanding AIC and BIC in model selection. *Sociol Methods Res* 33(2):261–304. <https://doi.org/10.1177/0049124104268644>
- Buschiazzo DE, Zobeck TM (2008) Validation of WEQ, RWEQ and WEPS wind erosion for different arable land management systems in the Argentinean pampas. *Earth Surf Process Landf* 33(12):1839–1850. <https://doi.org/10.1002/esp.1738>
- Callot Y, Marticorena B, Bergametti G (2000) Geomorphologic approach for modelling the surface features of arid environments in a model of dust emissions: application to the Sahara desert. *Geodin Acta* 13(5):245–270. <https://doi.org/10.1080/09853111.2000.11105373>
- Cao H, Liu J, Wang G, Yang G, Luo L (2015) Identification of sand and dust storm source areas in Iran. *J Arid Land* 7(5):567–578. <https://doi.org/10.1007/s40333-015-0127-8>
- Chadwick OA, Derry LA, Vitousek PM, Huebert BJ, Hedin LO (1999) Changing sources of nutrients during four million years of ecosystem development. *Nature* 397(6719):491–497. <https://doi.org/10.1038/17276>
- Chappell A, Sanderman J, Thomas M, Read A, Leslie C (2012) The dynamics of soil redistribution and the implications for soil organic carbon accounting in agricultural South-Eastern Australia. *Glob Change Biol* 18(6):2081–2088. <https://doi.org/10.1111/j.1365-2486.2012.02682.x>
- Chun Y, Boo KO, Kim J, Park SU, Lee M (2001) Synopsis, transport, and physical characteristics of Asian dust in Korea. *J Geophys Res: Atmos* 106(D16):18461–18469. <https://doi.org/10.1029/2001jd900184>
- Crucifix M, Hewitt CD (2005) Impact of vegetation changes on the dynamics of the atmosphere at the last glacial maximum. *Clim Dyn* 25(5):447–459. <https://doi.org/10.1007/s00382-005-0013-8>
- Gao Y, Arimoto R, Duce RA, Zhang XY, Zhang GY, An ZS, Chen LQ, Zhou MY, Gu DY (1997) Temporal and spatial distributions of dust and its deposition to the China sea. *Tellus B: Chem Phys Meteorol* 49(2):172–189. <https://doi.org/10.3402/tellusb.v49i2.15960>
- Ghaljahi M, Bagheri S, Keykhaei KR (2019) The effects of haze on general health of women employed in Zabol University of Medical Sciences in 2018. *Asian J Water, Environ Pollut* 16(2):59–64. <https://doi.org/10.3233/AJW190020>
- Ghorbani M (2013) *The economic geology of Iran*. Springer, Netherlands. <https://doi.org/10.1007/978-94-007-5625-0>
- Gill TE (1996) Eolian sediments generated by anthropogenic disturbance of playas: human impacts on the geomorphic system and geomorphic impacts on the human system. *Geomorphology* 17(1–3):207–228. [https://doi.org/10.1016/0169-555x\(95\)00104-d](https://doi.org/10.1016/0169-555x(95)00104-d)
- Ginoux P, Prospero JM, Gill TE, Hsu NC, Zhao M (2012) Global-scale attribution of anthropogenic and natural dust sources and their emission rates based on MODIS Deep Blue aerosol products. *Revi Geophys*. <https://doi.org/10.1029/2012rg000388>
- Goudie A, Middleton N (2001) Saharan dust storms: nature and consequences. *Earth Sci Rev* 56(1–4):179–204. [https://doi.org/10.1016/s0012-8252\(01\)00067-8](https://doi.org/10.1016/s0012-8252(01)00067-8)
- Goudie AS (2014) Desert dust and human health disorders. *Environ Int* 63:101–113. <https://doi.org/10.1016/j.envint.2013.10.011>
- Gregory JM, Wilson GR, Singh UB, Darwish MM (2004) TEAM: integrated, process-based wind-erosion model. *Environ Modell Softw* 19(2):205–215. [https://doi.org/10.1016/s1364-8152\(03\)00124-5](https://doi.org/10.1016/s1364-8152(03)00124-5)
- Hoffmann C, Funk R, Reiche M, Li Y (2011) Assessment of extreme wind erosion and its impacts in Inner Mongolia, China. *Aeolian Res* 3(3):343–351. <https://doi.org/10.1016/j.aeolia.2011.07.007>
- Husar RB, Tratt DM, Schichtel BA, Falke SR, Li F, Jaffe D, Gassó S, Gill T, Laulainen NS, Lu F et al (2001) Asian dust events of April 1998. *J Geophys Res: Atmos* 106(D16):18317–18330. <https://doi.org/10.1029/2000jd900788>

- Iqbal MJ, Ali M (2012) A probabilistic approach for estimating return period of extreme annual rainfall in different cities of Punjab. *Arab J Geosci* 6(7):2599–2606. <https://doi.org/10.1007/s12517-012-0548-z>
- Jickells TD (2005) Global iron connections between desert dust, ocean biogeochemistry, and climate. *Science* 308(5718):67–71. <https://doi.org/10.1126/science.1105959>
- Kamal A, Wu C, Lin Z (2019) Interannual variations of dust activity in western Iran and their possible mechanisms. *Big Earth Data*. <https://doi.org/10.1080/20964471.2019.1685825>
- Kaskaoutis D, Kosmopoulos P, Kambezidis H, Nastos P (2007) Aerosol climatology and discrimination of different types over Athens, Greece, based on Modis data. *Atmos Environ* 41(34):7315–7329. <https://doi.org/10.1016/j.atmosenv.2007.05.017>
- Khavarian-Garmsir AR, Pourahmad A, Hataminejad H, Farhoodi R (2019) Climate change and environmental degradation and the drivers of migration in the context of shrinking cities: a case study of Khuzestan province, Iran. *Sustain Cities Soc* 47:101480. <https://doi.org/10.1016/j.scs.2019.101480>
- Li J, Okin GS, Alvarez L, Epstein H (2007) Quantitative effects of vegetation cover on wind erosion and soil nutrient loss in a desert grassland of southern New Mexico, USA. *Biogeochemistry* 85(3):317–332. <https://doi.org/10.1007/s10533-007-9142-y>
- Liu X, Li N, Yuan S, Xu N, Shi W, Chen W (2015) The joint return period analysis of natural disasters based on monitoring and statistical modeling of multidimensional hazard factors. *Sci Total Environ* 538:724–732. <https://doi.org/10.1016/j.scitotenv.2015.08.093>
- Marticoarena B, Bergametti G, Gillette D, Belnap J (1997) Factors controlling threshold friction velocity in semiarid and arid areas of the United States. *J Geophys Res: Atmos* 102(D19):23277–23287. <https://doi.org/10.1029/97jd01303>
- Mesbahzadeh T, Mirakbari M, Mohseni Saravi M, Soleimani Sardoo F, Krakauer NY (2020a) Joint modeling of severe dust storm events in arid and hyper arid regions based on copula theory: a case study in the Yazd province, Iran. *Climate* 8(5):64. <https://doi.org/10.3390/cli8050064>
- Mesbahzadeh T, Salajeghe A, Sardoo FS, Zehtabian G, Ranjbar A, Marcello Miglietta M, Karami S, Krakauer NY (2020b) Spatial-temporal variation characteristics of vertical dust flux simulated by WRF-Chem model with GOCART and AFWA dust emission schemes (case study: Central Plateau of Iran). *Appl Sci* 10(13):4536. <https://doi.org/10.3390/app10134536>
- Middleton N (2017) Desert dust hazards: a global review. *Aeolian Res* 24:53–63. <https://doi.org/10.1016/j.aeolia.2016.12.001>
- Middleton N (2019) Variability and trends in dust storm frequency on decadal timescales: Climatic drivers and human impacts. *Geosciences* 9(6):261. <https://doi.org/10.3390/geosciences9060261>
- Middleton NJ (1986) A geography of dust storms in South-West Asia. *J Climatol* 6(2):183–196. <https://doi.org/10.1002/joc.3370060207>
- Mirakbari M, Mesbahzadeh T, Soleimani Sardoo F, Miglietta MM, Krakauer NY, Alipour N (2020) Observed and projected trends of extreme precipitation and maximum temperature during 1992–2100 in Isfahan province, Iran using REMO model and copula theory. *Nat Res Model*. <https://doi.org/10.1111/nrm.12254>
- Miri A, Ahmadi H, Ekhtesasi MR, Panjehkeh N, Ghanbari A (2009) Environmental and socio-economic impacts of dust storms in Sistan region, Iran. *Int J Environ Stud* 66(3):343–355. <https://doi.org/10.1080/00207230902720170>
- Modaresi Rad A, Khalili D, Kamgar-Haghighi AA, Zand-Parsa S, Banimahd SA (2016) Assessment of seasonal characteristics of streamflow droughts under semiarid conditions. *Nat Hazards* 82(3):1541–1564. <https://doi.org/10.1007/s11069-016-2256-6>
- Modarres R, Sadeghi S (2017) Spatial and temporal trends of dust storms across desert regions of Iran. *Nat Hazards* 90(1):101–114. <https://doi.org/10.1007/s11069-017-3035-8>
- Naderi M, Raeisi E (2015) Climate change in a region with altitude differences and with precipitation from various sources, South-Central Iran. *Theor Appl Climatol* 124(3–4):529–540. <https://doi.org/10.1007/s00704-015-1433-y>
- Nouri H, Faramarzi M, Sadeghi SH, Nasser S (2019) Effects of regional vegetation cover degradation and climate change on dusty weather types. *Environ Earth Sci*. <https://doi.org/10.1007/s12665-019-8763-5>
- Okin G, Gillette D, Herrick J (2006) Multi-scale controls on and consequences of Aeolian processes in landscape change in arid and semi-arid environments. *J Arid Environ* 65(2):253–275. <https://doi.org/10.1016/j.jaridenv.2005.06.029>
- Okin GS, Murray B, Schlesinger WH (2001) Degradation of sandy arid shrubland environments: observations, process modelling, and management implications. *J Arid Environ* 47(2):123–144. <https://doi.org/10.1006/jare.2000.0711>
- Overpeck J, Rind D, Lacs A, Healy R (1996) Possible role of dust-induced regional warming in abrupt climate change during the last glacial period. *Nature* 384(6608):447–449. <https://doi.org/10.1038/384447a0>

- Park SU (2003) Parameterization of dust emission for the simulation of the yellow sand (Asian dust) event observed in March 2002 in Korea. *J Geophys Res*. <https://doi.org/10.1029/2003jd003484>
- Peterson GA, Unger PW, Payne WA (2006) *Dryland agriculture*, 2nd edn. American Society of Agronomy, Madison
- Prospero JM (2002) Environmental characterization of global sources of atmospheric soil dust identified with the Nimbus 7 total Ozone Mapping Spectrometer (TOMS) absorbing aerosol product. *Revi Geophys*. <https://doi.org/10.1029/2000rg000095>
- Rashki A, Kaskaoutis D, Rautenbach C, Eriksson P, Qiang M, Gupta P (2012) Dust storms and their horizontal dust loading in the Sistan region, Iran. *Aeolian Res* 5:51–62. <https://doi.org/10.1016/j.aeolia.2011.12.001>
- Rashki A, Kaskaoutis D, Francois P, Kosmopoulos P, Legrand M (2015) Dust-storm dynamics over Sistan region, Iran: seasonality, transport characteristics and affected areas. *Aeolian Res* 16:35–48. <https://doi.org/10.1016/j.aeolia.2014.10.003>
- Reynolds R, Belnap J, Reheis M, Lamothe P, Luiszer F (2001) Aeolian dust in Colorado plateau soils: nutrient inputs and recent change in source. *Proc Natl Acad Sci* 98(13):7123–7127. <https://doi.org/10.1073/pnas.121094298>
- Schlesinger WH, Reynolds JF, Cunningham GL, Huenneke LF, Jarrell WM, Virginia RA, Whitford WG (1990) Biological feedbacks in global desertification. *Science* 247(4946):1043–1048. <https://doi.org/10.1126/science.247.4946.1043>
- Schneider von Deimling T, Ganopolski A, Held H, Rahmstorf S (2006) How cold was the last glacial maximum? *Geophys Res Lett*. <https://doi.org/10.1029/2006gl026484>
- Schwartz J (1994) Air pollution and daily mortality: a review and meta analysis. *Environ Res* 64(1):36–52. <https://doi.org/10.1006/enrs.1994.1005>
- Shao Y, Dong C (2006) A review on East Asian dust storm climate, modelling and monitoring. *Glob Planet Change* 52(1–4):1–22. <https://doi.org/10.1016/j.gloplacha.2006.02.011>
- Shao Y, Wang J (2003) A climatology of Northeast Asian dust events. *Meteorol Z* 12(4):187–196. <https://doi.org/10.1127/0941-2948/2003/0012-0187>
- Shao Y, Yang Y, Wang J, Song Z, Leslie LM, Dong C, Zhang Z, Lin Z, Kanai Y, Yabuki S et al (2003) Northeast Asian dust storms: real-time numerical prediction and validation. *J Geophys Res: Atmos*. <https://doi.org/10.1029/2003jd003667>
- Simonson RW (1995) Airborne dust and its significance to soils. *Geoderma* 65(1–2):1–43. [https://doi.org/10.1016/0016-7061\(94\)00031-5](https://doi.org/10.1016/0016-7061(94)00031-5)
- Smyth D (2018) Q&A: climate change in Iran by fast-emerging photographer Hashem Shakeri. *Br J Photogr* <https://www.bjp-online.com/2018/09/hashem-shakeri/>
- UNEP, WMO, UNCCD (2016) *Global assessment of sand and dust storms*. Tech Rep
- Webb NP, McGowan HA, Phinn SR, Leys JF, McTainsh GH (2009) A model to predict land susceptibility to wind erosion in Western Queensland, Australia. *Environ Modell Softw* 24(2):214–227. <https://doi.org/10.1016/j.envsoft.2008.06.006>

Publisher's Note Springer Nature remains neutral with regard to jurisdictional claims in published maps and institutional affiliations.